J Fluoresc (2013) 23:1007–1018
DOI 10.1007/s10895-013-1227-5

ORIGINAL PAPER

Development of UV-Excitable Red and Near-Infrared Fluorescent Labels and Their Application for Simultaneous Multicolor Bioimaging by Single-Wavelength Excitation

Tetsuya Mizuno · Keitaro Umezawa · Yutaka Shindo · Daniel Citterio · Kotaro Oka · Koji Suzuki

Received: 16 January 2013 / Accepted: 30 April 2013 / Published online: 23 May 2013

Abstract We report a new type of UV-excitable red/NIR-emissive fluorescent dyads (PKF series). Conjugation of a pyrene and a novel bright red/near-infrared (NIR) fluorophore resulted in large quasi-Stokes shift while retaining intense fluorescence emission and sharp spectral bands. Labeling of PKF dyads to biomolecules was performed by means of introduction of a succinimidyl ester. Simultaneous Ca^{2+}/albumin dual-color intracellular imaging by PKF in combination with fura-2 (UV-excitable/VIS-emissive Ca^{2+} indicator) reveals its usefulness as a new bioimaging tool.

Keywords Bioimaging · BODIPY · Fluorescent dyads · Near-infrared fluorophore

Introduction

Multicolor fluorescent bioimaging by *single-wavelength excitation* has been recently spotlighted as a powerful tool for real-time simultaneous monitoring of multiple targets in cells with high temporal resolution (without time delay caused by switching of excitation wavelength), which is expected to enable the visualization and comprehension of fast signal dynamics or signal changes in highly motile cells. For this aim, several pairs of genetically encoded fluorescence resonance energy transfer (FRET) sensors (dual-FRET sensors) excitable by a Xe lamp or a violet laser (405 nm) have been developed, and simultaneous imaging of cAMP/cGMP or Ca^{2+}/caspase-3 by single-wavelength excitation has been demonstrated [1, 2]. However, due to their broad emission spectra, these fluorescent protein (FP)-based FRET sensors fully occupy the spectral region between 400 and 600 nm, which restricts their further use with other fluorescent probes. On the other hand, the far-red or near-infrared (NIR) region [3] (>650 nm) remains available for imaging purposes, because many of the FPs do not exhibit strong emission at these wavelengths, indicating that the efficient use of this spectral region is of considerable interest to overcome the current limitation.

Organic fluorescent probes have advantages over FPs in terms of spectral variation from the ultra-violet (UV) to the NIR, spectral sharpness and brightness. Therefore, it was considered that the development of new types of fluorescent low molecular weight compounds would further push forward the simultaneous multicolor imaging research field. However, their relatively small Stokes shift (usually <50 nm) is an issue still remaining to be improved. On the other hand, the Megastokes dyes®, which are known to have large Stokes shifts over 100 nm, show broad emission spectra (full width at half maximum height: $\Delta\lambda_{1/2}$~100 nm) (http://www.dyomics.com/megastokes-dyes.html), causing signal crosstalk during multicolor bioimaging. Investigation of phosphorescent heavy-metal complexes is actually one of the approaches towards large-Stokes-shift emitters, but some drawbacks such as toxicity, low extinction coefficients or fluorescence quenching by water are sometimes encountered, which are now research targets for improvement [4].

Another way to enlarge Stokes shifts, the concept of organic fluorescent molecular dyads (often also referred to

T. Mizuno · D. Citterio · K. Suzuki (✉)
Department of Applied Chemistry, Faculty of Science and Technology, Keio University, 3-14-1, Hiyoshi, Kohoku-ku, Yokohama 223-8522, Japan
e-mail: suzuki@applc.keio.ac.jp

K. Umezawa · Y. Shindo · K. Oka
Department of Bioinformatics, Faculty of Science and Technology, Keio University, 3-14-1, Hiyoshi, Kohoku-ku, Yokohama 223-8522, Japan

as energy transfer cassettes or molecular cassettes), has been investigated [5]. Two fluorescent molecules (energy donor and acceptor) covalently connected by a rigid and short linker (e.g. alkyne) undergo fast intramolecular energy transfer from the donor to the acceptor [6]. On the basis of this mechanism, several types of "donor–acceptor" energy transfer cassettes, which have large quasi-Stokes shifts (λ_{flu}–λ_{abs}), have been developed [6–22]. Additionally, the application of such cassettes for intracellular imaging is an interesting but still challenging theme [14, 17, 21, 22]. Herein, we report a new class of molecular cassettes (PKF: Pyrene–Keio Fluor cassettes, Fig. 1) with high optical performance, and their application for real-time simultaneous imaging of multiple targets in cells in combination with visible-light (VIS)-emissive fluorescent probes.

Experimental

Synthesis

General Regards

All chemical reagents and solvents for synthesis were purchased from commercial suppliers (Wako Pure Chemical, Tokyo Kasei Industry and Aldrich Chemical) and were used without further purification. All solvents for HPLC were purchased from Wako Pure Chemical and Kanto Chemical. All moisture-sensitive reactions were carried out under an atmosphere of argon. The composition of mixed solvents is given as volume ratio (*v*/*v*).

^{1}H NMR and ^{13}C NMR spectra were recorded on a Varian MVX-300 (Varian Inc.) or an ECA-500 (JEOL Ltd.) spectrometer at room temperature. The measurements for 1H NMR and 13C NMR were performed at 300 MHz (MVX-300) or 500 MHz (ECA-500), and 75 MHz (MVX-300) or 125 MHz (ECA-500), respectively. All chemical shifts are relative to an internal standard of tetramethylsilane (δ=0.0 ppm), and coupling constants are given in Hz. Flash chromatography separation was undertaken using a YFLC-Al-560 chromatograph (Yamazen Co. Ltd.). HPLC purification was performed by a recycle HPLC LC-918 (Japan Analytical Industry) equipped with a reversed-phase (RP) column Inertsil ODS-3 (30×50 mm) (GL Sciences Inc.) for RP-HPLC, or two gel permeation chromatograph (GPC) columns JAIGEL-1H, 2H (Japan Analytical Industry) for GPC, respectively. High-resolution mass spectra (HRMS, electrospray ionization: ESI) were recorded on a MicrOTOF (Bruker Ltd.).

The following abbreviations are used in this manuscript: DMAP: N,N-dimethyl-4-aminopyridine, DCC: *N,N*-dicyclohexylcarbodiimide, EDC: 1-ethyl-3-(3-dimethylaminopropyl) carbodiimide hydrochloride; DIEA: *N,N*-diisopropylethylamine TEA: triethylamine, DMF: *N,N*-dimethylformamide, THF: tetrahydrofuran, TFA: trifluoroacetic acid. Compounds 3a, 3b, and 3c were synthesized according to previously reported literature [23].

2-Methyl-4-pyren-1-yl-but-3-yn-2-ol 1

1-Bromopyrene (506 mg, 1.80 mmol, 1 eq.), 2-methyl-3-buten-2-ol (1.19 g, 14.1 mmol, 8 eq.), CuI (I) (126 mg, 0.661 mmol, 0.3 eq.), and triphenylphosphine (193 mg, 0.735 mmol, 0.4 eq.) were dissolved in toluene (8 ml) and TEA (30 ml), and the solution was degassed *in vacuo* and purged with nitrogen gas. Dichloro[1,1′-bis(diphenylphosphino)ferrocene] palladium (II) dichloromethane complex (1:1) (100 mg, 0.122 mmol, 0.1 eq.) was added to the reaction mixture and stirred at 80 °C overnight. After cooling to room temperature, saturated NH_4Cl aqueous solution was added, and the resulting aqueous phase was extracted with toluene. The combined organic phase was washed with brine, dried over Na_2SO_4, filtered and evaporated. The resulting residue was purified by column chromatography (silica gel, *n*-hexane/CH_2Cl_2=30/70 to 10/90) to obtain 2-methyl-4-pyren-1-yl-but-3-yn-2-ol (510 mg, 99 %) as a white powder. ^{1}H-NMR (500 MHz, $CDCl_3$): δ (ppm)=8.40 (d, *J*= 9.0 Hz, 1H), 8.07–7.84 (m, 8H), 2.65 (s, 1H), 1.79 (s, 6H). ^{13}C-NMR (500 MHz, $CDCl_3$): δ (ppm)=132.0, 131.3, 131.2, 131.0, 129.7, 128.4, 128.1, 127.2, 126.2, 125.64, 125.59, 125.4, 124.44, 124.40, 124.3, 117.2, 99.6, 81.4, 66.2, 31.9.

1-Ethynylpyrene 2

To a solution of 2-methyl-4-pyren-1-yl-but-3-yn-2-ol (510 mg, 1.80 mmol, 1 eq.) in toluene (150 ml) was added KOH (387 mg, 6.89 mmol, 4 eq.), and stirred at 80 °C for 3 h. After cooling to room temperature, the reaction solution was washed with water and brine, dried over Na_2SO_4, filtered and evaporated. The resulting residue was purified by column chromatography (silica gel, *n*-hexane/CH_2Cl_2=80/20 to

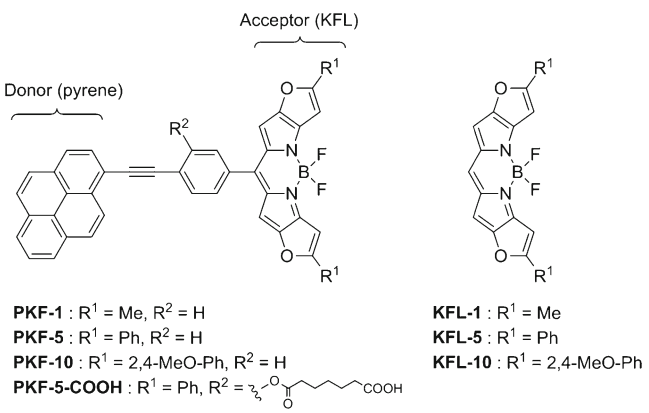

Fig. 1 Chemical structures of PFKs and KFLs

50/50) to obtain 1-ethynylpyrene (353 mg, 87 %) as a white powder. ^{1}H-NMR (500 MHz, $CDCl_3$): δ (ppm)=8.51 (d, J= 9.2 Hz, 1H), 8.13–8.06 (m, 4H), 8.00–7.90 (m, 4H), 3.59 (s, 1H). ^{13}C-NMR (500 MHz, $CDCl_3$): δ (ppm)=132.4, 131.5, 131.0, 130.8, 130.0,128.4, 128.3, 127.0, 126.1, 125.6, 125.6, 125.2, 124.3, 124.2, 124.0, 116.4, 82.7, 82.5.

Compound 5a

2-Methyl-4*H*-furo[3,2-*b*]pyrrole-5-carboxylic acid 3a (168 mg, 1.02 mmol, 2 eq.) was dissolved in TFA (2 ml) and stirred at 50 °C for 40 min. 4-Iodobenzaldehyde (118 mg, 0.509 mmol, 1 eq.) in TFA (2 ml) and methanesulfonic acid (0.2 ml) were added to the reaction mixture and stirred overnight at room temperature. *p*-Chloranil (128 mg, 0.521 mmol, 1 eq.) was added to the solution and the stirring was further continued for 90 min. The reaction mixture was slowly poured into saturated $NaHCO_3$ aqueous solution (100 ml), and the resulting aqueous solution was extracted with CH_2Cl_2. The collected organic phase was washed with water and brine, dried over Na_2SO_4 and evaporated. The resulting residue was purified by column chromatography (alumina, *n*-hexane/chloroform =30/70) to obtain 4a (160 mg, 0.352 mmol). The compound 4a was dissolved in CH_2Cl_2 (10 ml), and TEA (0.5 ml) and BF_3 Et_2O complex (0.5 ml) were added to the reaction solution, and stirred for 2 h at room temperature. The reaction mixture was diluted with toluene, washed with saturated $NaHCO_3$ aqueous solution and brine, dried over Na_2SO_4 and evaporated. The resulting residue was purified by chromatography (silica gel, eluent: *n*-hexane/chloroform =50/50 to 25/75) to obtain 5a as a yellow metallic solid (74.1 mg, 29 % for 2 steps). ^{1}H NMR (300 MHz, $CDCl_3$): δ (ppm)=7.84 (d, J=8.1 Hz, 2H), 7.27 (d, J=8.4 Hz, 2H), 6.35 (s, 2H), 6.13 (s, 2H), 2.46 (s, 6H). ^{13}C NMR (500 MHz, $CDCl_3$): δ (ppm)=169.5, 153.1, 150.3, 142.3, 137.5, 137.5, 133.8, 132.1, 103.1, 97.9, 96.1, 15.8.

Compound 5b

2-Phenyl-4*H*-furo[3,2-*b*]pyrrole-5-carboxylic acid 3b (202 mg, 0.89 mmol, 2 eq.) was dissolved in TFA (4 ml) and stirred at 40 °C for 30 min. 4-Iodobenzaldehyde (103 mg, 0.445 mmol, 1 eq.) in TFA (1 ml) and methanesulfonic acid (0.1 ml) were added to the reaction mixture and stirred overnight at room temperature. *p*-Chloranil (118 mg, 0.481 mmol, 1.1 eq.) was added to the solution and the stirring was further continued for 1 h. The reaction mixture was slowly poured into saturated $NaHCO_3$ aqueous solution (100 ml), and the resulting aqueous solution was extracted with CH_2Cl_2. The collected organic phase was washed with water and brine, dried over Na_2SO_4 and evaporated. The resulting residue was purified by column chromatography (alumina, *n*-hexane/chloroform =30/70) to obtain 4b (179 mg, 0.309 mmol). The compound 4b was dissolved in CH_2Cl_2 (10 ml), and DIEA (0.3 ml) and BF_3 Et_2O complex (0.3 ml) were added to the reaction solution, and stirred for 1 h at room temperature. The reaction mixture was diluted with toluene, washed with saturated $NaHCO_3$ aqueous solution and brine, dried over Na_2SO_4 and evaporated. The resulting residue was purified by chromatography (silica gel, eluent: *n*-hexane/chloroform =50/50 to 25/75) to obtain 5b as a yellow metallic solid (112 mg, 40 % for 2 steps). ^{1}H NMR (300 MHz, $CDCl_3$): δ (ppm)=7.88 (d, J=8.4 Hz, 2H), 7.83 (dd, J=1.2 Hz, 7.8 Hz, 4H), 7.50–7.42 (m, 6H), 7.33 (d, J=8.7 Hz, 2H), 7.01 (s, 2H), 6.27 (s, 2H). ^{13}C NMR (500 MHz, $CDCl_3$): δ (ppm)= 168.1, 153.9, 150.1, 141.1 139.3, 137.7, 133.8, 132.2, 130.3, 129.7, 129.1, 125.6, 103.2, 96.3, 95.6.

Compound 5c

2-(2,4-Dimethoxyphenyl)-4*H*-furo[3,2-*b*]pyrrole-5-carboxylic acid 3c (410 mg, 1.43 mmol, 2 eq.) was dissolved in TFA (5 ml) and stirred at 40 °C for 20 min. 4-Iodobenzaldehyde (165 mg, 0.713 mmol, 1 eq.) in TFA (2 ml) and methanesulfonic acid (0.3 ml) were added to the reaction mixture and stirred overnight at room temperature. *p*-Chloranil (182 mg, 0.738 mmol, 1 eq.) was added to the solution and the stirring was further continued for 1 h. The reaction mixture was slowly poured into saturated $NaHCO_3$ aqueous solution (200 ml), and the resulting aqueous solution was extracted with CH_2Cl_2. The collected organic phase was washed with water and brine, dried over Na_2SO_4 and evaporated. The resulting residue was purified by column chromatography (alumina, *n*-hexane/chloroform=30/70) to obtain 4c (348 mg, 0.497 mmol). The compound 4c was dissolved in CH_2Cl_2 (30 ml), and DIEA (0.7 ml) and BF_3 Et_2O complex (0.7 ml) were added to the reaction solution, and stirred for 90 min at room temperature. The reaction mixture was diluted with toluene, washed with saturated $NaHCO_3$ aqueous solution and brine, dried over Na_2SO_4 and evaporated. The resulting residue was purified by chromatography (silica gel, eluent: *n*-hexane/chloroform=40/60 to 20/80) to obtain 5c as a yellow metallic solid (96.6 mg, 18 % for 2 steps). ^{1}H NMR (500 MHz, THF-d_8): δ (ppm)=7.92 (d, J=8.3 Hz, 2H), 7.86 (d, J=8.9 Hz, 2H), 7.42 (d, J=8.6 Hz, 2H), 7.09 (s, 2H), 6.68 (d, J=2.3 Hz, 2H), 6.64 (dd, J=8.9 Hz, 2.3 Hz, 2H), 6.24 (s, 2H), 4.03 (s, 6H), 3.86 (s, 6H). ^{13}C NMR (500 MHz, THF-d_8): δ (ppm)= 166.7, 165.7, 160.0, 153.4, 151.6, 140.2, 140.0, 138.5, 135.5, 133.4, 129.0, 112.9, 106.7, 102.0, 99.5, 99.0, 96.4, 56.0, 55.8.

PKF-1

Compound 5a (33.7 mg, 0.093 mmol, 1 eq.), 1-ethynylpyrene (30.8 mg, 0.131 mmol, 1.5 eq.), and CuI(I)

(23.0 mg, 0.121 mmol, 1.4 eq) were dissolved in DMF (8 ml) and DIEA (1.2 ml), and degassed *in vacuo*. Tetrakis(triphenylphosphine)palladium(0) (40.0 mg, 0.034 mmol, 0.3 eq.) was added to the reaction mixture and stirred at room temperature for 2.5 h. 1N HCl aqueous solution was added to the reaction mixture, and the aqueous solution was extracted with toluene. The combined organic phase was washed with water and brine, dried over Na_2SO_4, filtered and evaporated. The resulting residue was purified by column chromatography (silica gel, *n*-hexane/chloroform= 50/50 to 20/80) and GPC (chloroform) to obtain PKF-1 (1.2 mg, 2 %) as a golden metallic solid. ^{1}H-NMR (300 MHz, $CDCl_3$): δ (ppm)=8.70 (d, J=9.0 Hz, 1H), 8.28–8.04 (m, 8H), 7.85 (d, J=7.8 Hz, 2H), 7.63 (d, J=7.8 Hz, 2H), 6.38 (s, 2H), 6.24 (s, 2H), 2.49 (s, 6H). HRMS-ESI (*m/z*): $[M+Na]^+$ calculated for $C_{39}H_{23}BF_2N_2NaO_2^+$: 623.1720; found: 623.1700 (1.9 mDa, 3.0 ppm).

PKF-5

Compound 5b (28.0 mg, 0.045 mmol, 1 eq.), 1 ethynylpyrene (14.4 mg, 0.064 mmol, 1.2 eq.), and CuI(I) (7.7 mg, 0.040 mmol, 1 eq) were dissolved in DMF (5 ml) and DIEA (1 ml), and degassed *in vacuo*. Tetrakis(triphenylphosphine)palladium(0) (20.0 mg, 0.017 mmol, 0.3 eq.) was added to the reaction mixture and stirred at room temperature for 2 h. 1N HCl aqueous solution was added to the reaction mixture, and the aqueous solution was extracted with toluene. The combined organic phase was washed with water and brine, dried over Na_2SO_4, filtered and evaporated. The resulting residue was purified by column chromatography (silica gel, *n*-hexane/chloroform=40/60 to 10/90), and GPC (chloroform) to obtain PKF-5 (8.0 mg, 25 %) as a golden metallic solid. ^{1}H-NMR (500 MHz, $CDCl_3$): δ (ppm)=8.72 (d, J=8.9 Hz, 1H), 8.28–8.07 (m, 8H), 7.90–7.84 (m, 5H), 7.69–7.67 (m, 3H), 7.49–7.43 (m, 6H), 7.04 (s, 2H), 6.38 (s, 2H). HRMS-ESI (*m/z*): $[M+Na]^+$ calculated for $C_{49}H_{27}BF_2N_2NaO_2^+$: 747.2034; found: 747.2031 (0.3 mDa, 0.4 ppm).

PKF-10

Compound 5c (6.4 mg, 0.009 mmol, 1 eq.), 1 ethynylpyrene (3.1 mg, 0.014 mmol, 1.5 eq.), and CuI(I) (1.0 mg, 0.005 mmol, 0.5 eq) were dissolved in 1,4-dioxane (2 ml) and TEA (0.1 ml), and degassed *in vacuo*. Tetrakis(triphenylphosphine)palladium(0) (10.0 mg, 0.008 mmol, 1 eq.) was added to the reaction mixture and stirred at room temperature for 4.5 h. The reaction solution was evaporated and the resulting residue was purified by column chromatography (silica gel, *n*-hexane/chloroform= 50/50 to 20/80), and GPC (chloroform) to obtain PKF-10 (2.0 mg, 28 %) as a golden metallic solid. ^{1}H-NMR (500 MHz, $CDCl_3$): δ (ppm)=8.72 (d, J=9.0 Hz, 1H), 8.28–8.04 (m, 10H), 7.92 (d, J=8.8 Hz, 2H), 7.86 (d, J= 8.0 Hz, 2H), 7.68 (d, J=7.8 Hz, 2H), 6.60 (d, J=9.0 Hz, 2H), 6.56 (s, 2H), 6.26 (s, 2H), 3.94 (s, 6H), 3.84 (s, 6H). HRMS-ESI (*m/z*): $[M+Na]^+$ calculated for $C_{53}H_{35}BF_2N_2NaO_6^+$: 867.2457; found: 867.2459 (−0.2 mDa, −0.2 ppm).

Compound 5d

2-Phenyl-4*H*-furo[3,2-*b*]pyrrole-5-carboxylic acid 3c (147 mg, 0.648 mmol, 2 eq.) was dissolved in TFA (2 ml) and stirred at 40 °C for 40 min. 3-Hydroxy-4-iodobenzaldehyde (78.8 mg, 0.318 mmol, 1 eq.) in TFA (1.5 ml) and methanesulfonic acid (0.15 ml) were added to the reaction mixture and stirred overnight at room temperature. *p*-Chloranil (88.5 mg, 0.360 mmol, 1 eq.) was added to the solution and the stirring was further continued for 2 h. The reaction mixture was slowly poured into saturated $NaHCO_3$ aqueous solution (200 ml), and the resulting aqueous solution was extracted with CH_2Cl_2. The collected organic phase was washed with water and brine, dried over Na_2SO_4 and evaporated. The resulting residue was purified by column chromatography (alumina, *n*-hexane/chloroform =30/70) to obtain 4d (125 mg, 0.211 mmol). The compound 4d was dissolved in CH_2Cl_2 (20 ml), and DIEA (0.4 ml) and BF_3 Et_2O complex (0.4 ml) were added to the reaction solution, and stirred for 1 h at room temperature. The reaction mixture was diluted with toluene, washed with saturated $NaHCO_3$ aqueous solution and brine, dried over Na_2SO_4 and evaporated. The resulting residue was purified by chromatography (silica gel, eluent: *n*-hexane/chloroform =45/55 to 10/90) to obtain 5d as a yellow metallic solid (38.7 mg, 19 % for 2 steps). ^{1}H NMR (300 MHz, $CDCl_3$): δ (ppm)=7.83–7.77 (m, 5H), 7.49–7.41 (m, 6H), 7.18 (d, J= 2.1 Hz, 1H), 6.99 (s, 2H), 6.88 (dd, J=2.1 Hz, 8.1 Hz, 1H), 6.30 (s, 2H), 5.75 (s, 1H).

PKF-5-OH

Compound 5d (45.3 mg, 0.067 mmol, 1 eq.), 1-ethynylpyrene (32.6 mg, 0.144 mmol, 2.5 eq.), and CuI(I) (2.0 mg, 0.011 mmol, 0.2 eq) were dissolved in THF (5 ml) and TEA (1.25 ml), and degassed *in vacuo*. *trans*-Dichlorobis(triphenylphosphine)palladium(II) (20.0 mg, 0.028 mmol, 0.3 eq.) was added to the reaction mixture and stirred at 45 °C for 1.5 h. Saturated NH_4Cl aqueous solution was added to the reaction mixture, and the resulting aqueous solution was extracted with toluene. The combined organic phase was washed with brine, dried over Na_2SO_4, filtered and evaporated. The resulting residue was purified by preparative thin layer chromatography (silica gel, *n*-

hexane/chloroform=5/95) to obtain PKF-5-OH (13.4 mg, 27 %) as a golden metallic solid. ^{1}H-NMR (300 MHz, $CDCl_3$): δ (ppm)=8.64 (d, J=9.3 Hz,1H), 8.29–8.08 (m, 8H), 7.86–7.82 (m, 4H), 7.76 (d, J=8.1 Hz, 1H) 7.50–7.42 (m, 6H), 7.33 (d, J=1.5 Hz, 1H), 7.03 (d, J=0.9 Hz, 2H), 6.43 (s, 2H), 6.25 (s, 1H).

PKF-5-COOH

PKF-5-OH (5.9 mg, 0.008 mmol, 1 eq.), pimelic acid (12.7 mg, 0.079 mmol, 10 eq.) and DMAP (1 mg, 0.009 mmol, 1 eq.) were dissolved in THF (1.5 ml) on ice. DCC (5.1 mg, 0.025 mmol, 3 eq.) was added to the reaction mixture at the same temperature and the solution was warmed up to room temperature and stirred for 1 h. Saturated NH_4Cl aqueous solution was added to the reaction mixture, and the resulting aqueous solution was extracted with CH_2Cl_2. The combined organic phase was washed with brine, dried over Na_2SO_4, filtered and evaporated. The resulting residue was purified by column chromatography (silica gel, chloroform/methanol=99/1 to 90/10), and RP-HPLC (acetone/methanol=80/20) to obtain PKF-5-COOH (2.4 mg, 34 %) as a purple solid. ^{1}H-NMR (500 MHz, THF-d_8): δ (ppm)=8.74 (d, J=8.9 Hz, 1H), 8.34–8.32 (m, 2H), 8.29–8.26 (m, 3H), 8.16 (dd, J=8.9 Hz, 2.6 Hz, 2H), 8.07 (t, J=7.8 Hz, 1H), 7.99–7.97 (m, 5H), 7.69 (d, J=7.7 Hz, 2H), 7.49–7.47 (m, 4H), 7.43–7.40 (m, 2H), 7.27 (s, 2H), 6.57 (s, 2H), 2.84–2.81 (m, 2H), 2.17–2.13 (m, 2H), 1.89–1.82 (m, 2H), 1.59–1.55 (m, 2H), 1.50–1.45 (m, 2H). HRMS-ESI (m/z): $[M+Na]^+$ calculated for $C_{56}H_{37}BF_2N_2NaO_6^+$: 905.2614; found: 905.2608 (0.6 mDa, 0.6 ppm).

Measurement

All solvents for spectrometry were purchased from Kanto Chemical. Absorption spectra were recorded on a Hitachi U-2001 double beam spectrophotometer (Hitachi, Tokyo, Japan). Fluorescence emission spectra, 3D fluorescence/emission spectra and quantum yields were recorded on a SREX Fluorolog-3 (Model FL-3–11, Horiba Jobin Yvon, Kyoto, Japan) equipped with a R2658P photomultiplier tube (Hamamatsu Photonics, Shizuoka, Japan) as a fluorescence detector, or on a F-4500 fluorophotometer (Hitachi Co., Tokyo, Japan) at 25 °C. Measurements of quantum yields were performed by following the method recommended by Horiba Jobin Yvon (see: http://www.jp.jobinyvon.horiba.com/product_j/spex/quantum_yield/img/quantum_yields.pdf). A number of diluted solutions of different dye concentrations (A<0.10, to prevent reabsorption) were prepared, and the absorbance (A) and the integrated fluorescence intensity (F) at each concentration were recorded. Then a graph of F versus A was plotted to determine the gradient (*Grad*). Quantum yields ϕ were calculated by using Eq. (1):

$$\Phi_{sample} = \Phi_{ref} \cdot \left(\frac{Grad_{sample}}{Grad_{ref}}\right) \cdot \left(\frac{n_{sample}}{n_{ref}}\right)^2 \quad (1)$$

The subscripts *ref* and *sample* denote the reference dye and the sample, respectively, and n is the refractive index of the solvent. $\phi_{D\text{-}A}$ and $\phi_{A\text{-}A}$ denote the quantum yields by irradiation in the pyrene (donor) and KFL (acceptor) unit, respectively. The following reference dyes were used: Quinine sulfate (ϕ=0.55 in 0.5 M H_2SO_4 solution) [24] for all dyes ($\phi_{D\text{-}A}$), cresyl violet (ϕ=0.54 in methanol) [25] for PKF-1 ($\phi_{A\text{-}A}$), 3,3′-diethyl-thiadicarbocyanine (ϕ=0.35 in ethanol) [26] for PKF-5 and PKF-5-COOH ($\phi_{A\text{-}A}$), KFL-10 (ϕ=0.81 in chloroform) [27] for PKF-10 ($\phi_{A\text{-}A}$).

Protein Labeling

Synthesis of PKF-5-NHS Ester

To a solution of PKF-5-COOH (2.1 mg, 0.002 mmol) and *N*-hydroxysuccinimide (7.1 mg, 0.061 mmol) in THF (1 ml) was added EDC (12.6 mg, 0.061 mmol) and stirred overnight. Saturated $NaHCO_3$ aqueous solution was added to the reaction mixture and the resulting solution was extracted with CH_2Cl_2. The organic phase was washed with brine, dried over Na_2SO_4, filtered and evaporated. The resulting residue was purified by preparative thin layer chromatography (silica, *n*-hexane/chloroform=85/15) to obtain PKF-5-NHS ester, which was dissolved in DMF (1.5 ml) for storage in the freezer. PKF-5-NHS ester solution was used for the next protein conjugation.

Labeling of PKF-5-NHS to Protein

Stock solutions of protease free bovine serum albumin (BSA) (80 mg) dissolved in PBS buffer (pH=7.4, 8 ml), and pluronic F-127 (210 mg, nonionic surfactant polyol (http://probes.invitrogen.com/media/pis/mp03000.pdf)) in DMF (1 ml) were prepared. PKF-5-NHS ester solution (50 μl) was added to the mixture of one aliquot of BSA solution (850 μl) and of pluronic F-127 solution (100 μl), and stirred at room temperature for 2 h. The reaction mixture was purified by PD-10 columns Sephadex™ G-25M (GE Healthcare) and the resulting fraction was lyophilized to obtain BSA-PKF-5 as a green powder.

Cell Culture

HUVEC were purchased from Sanko Junyaku (Tokyo, Japan) and cultured in endothelial growth medium-2 (EGM-2) (Lonza, Walkersville, MD, USA). For

experimental use, HUVEC were cultured on glass bottom dishes (Iwaki, Tokyo, Japan) coated with collagen. Cultures were maintained at 37 °C in a humidified atmosphere of 5 % CO_2.

Fluorescent Imaging

For fluorescent measurements, cells were incubated with 10 mg/ml PKF-albumin as mixtures with pluronic F-127 (Invitrogen, Carlsbad, CA, USA) in Hanks' balanced salt solutions (HBSS) containing (in mM): NaCl, 137; KCl, 5.4; $CaCl_2$, 1.3; $MgCl_2$, 0.5; $MgSO_4$, 0.4; Na_2HPO_4, 0.3; KH_2PO_4, 0.4; $NaHCO_3$, 4.2; D-Glucose, 5.6; HEPES, 5 (pH adjusted to 7.4 with NaOH) for 1 h at 37 °C, and then washed twice with HBSS. For simultaneous imaging of PKF-albumin and intracellular Ca^{2+}, PKF-albumin loaded cells were further incubated with 20 nM fura-2 AM in HBSS for 30 min at 37 °C. Then, cells were washed twice and further incubated for 15 min for complete hydrolysis of the acetoxymethyl ester. These dyes were excited at 380 nm. Fluorescence images were acquired with an inverted microscope (ECLIPSE TE300, Nikon, Tokyo, Japan) equipped with a 20× objective lens (S Fluor, Nikon) and a 400 nm dichroic mirror. Signals from PFK-albumin and fura-2 were separated using a 590 nm dichroic mirror and passed through a 600 nm long pass filter and 535/55 band pass filter, respectively. A 150 W Xe lamp with a monochromator unit was used for excitation, and fluorescence was measured with a CCD camera (HiSCA, Hamamatsu Photonics).

Results and Discussion

Molecular Design and Synthesis of PKF Series

The fluorescent dyads of the PKF series consist of two units (energy acceptor and donor) as shown in Fig. 1. As energy acceptors, boron-dipyrromethene (BODIPY)-based long-wavelength emitting fluorophores (KFL) were selected due to their following features: 1) high fluorescence quantum yields (up to 98 %), 2) sharp emission spectral bands ($\Delta\lambda_{1/2}$ <30 nm), 3) large emission spectral variation (547–738 nm), as well as large extinction coefficients [23, 27]. It was assumed that these features would allow multicolor imaging in combination with other VIS-emissive fluorescent probes without significant signal crosstalk [28]. Therefore, three KFL dyes (KFL-1, KFL-5, KFL-10) with emission peaks around 590 nm, 650 nm and 690 nm, respectively, have been chosen [23]. As energy donor, a pyrene moiety was chosen, because its absorption spectral band (around 400 nm) is compatible with commercially available excitation sources for fluorescence microscopy (e.g. Xe lamp, mercury lamp, violet laser: 405 nm). Furthermore, a rigid ethynylene linker was expected to invoke fast intramolecular energy transfer from the donor to the second electronically excited (S_2) level of the acceptor [11], while preventing intramolecular electrostatic quenching [6]. The designed PKFs were synthesized following a straightforward synthetic route (Fig. 2): each of the synthesized building blocks (pyrene-acetylene and PKF-iodide) could be conjugated with each other by Sonogashira cross-coupling under mild condition.

Optical Properties of PKF Dyads

As shown in Table 1 and Fig. 3, separate absorption bands for the pyrene unit (ε_{pyrene}: ca. 40,000 $M^{-1}cm^{-1}$) and the KFL unit (ε_{KFL}: 141,000–160,000 M^{-1} cm^{-1}) were observed. Excitation of the PKFs at 365 nm resulted in the appearance of fluorescence emission bands at around 600 nm, 670 nm, and 715 nm, respectively, whereas no emission corresponding to the pyrene fluorophore (~400 nm) was observed. The absorption spectra of KFL-1, -5, and -10, which do not have a pyrene unit, exhibited weak absorption and excitation bands around 400 nm, which are considered to correspond to the S_0–S_2 transitions of the fluorophores (Fig. 4). 3D-Excitation/emission spectra of these dyes (Fig. 5) revealed that these dyads could be excited in the UV-violet wavelength range. Furthermore, the emission intensity of PKFs excited at around 350–400 nm is increased in comparison to those of KFLs, implying that an intramolecular energy transfer from the pyrene to the KFL unit occurs. A similar phenomenon was observed in case of pyrene–BODIPY cassettes, and it was concluded to be due to the energy transfer from the donor to the S_2 level of the acceptor [11]. Therefore, it is presumably reasonable that the S_0–S_2 transition band of KFL contributes to the energy transfer from pyrene to KFL, hence making PKFs work as energy cassettes.

The fluorescence spectral bands of the dyes of the PFK series are remarkably sharp ($\Delta\lambda_{1/2}$<30 nm) with low spectral overlap being observed among the three dyes. This fact is attributed to the structural planarity of the KFL cores, which differs from other phenyl-substituted BODIPY dyes as previously discussed in the literature [27]. In fact, similar pyrene-BODIPY (NIR) cassettes exhibited relatively broad spectral peaks ($\Delta\lambda_{1/2}$=50–80 nm), causing larger spectral overlap [12]. This result indicates that the light emitted by the PKFs can be very efficiently collected by a detector through narrow filters. The fluorescence quantum yields of PKF-5 and -10 obtained by excitation of the KFL unit ($\phi_{A\text{-}A}$) are very high (86 and 65 %, respectively), retaining the original optical properties of KFL-5 and -10 themselves (90 % and 81 %, respectively) [23]. In contrast, only the quantum yield of PKF-1 excited at 570 nm ($\phi_{A\text{-}A}$: 28 %) is exceptionally lower than that of KFL-1 itself (96 %).

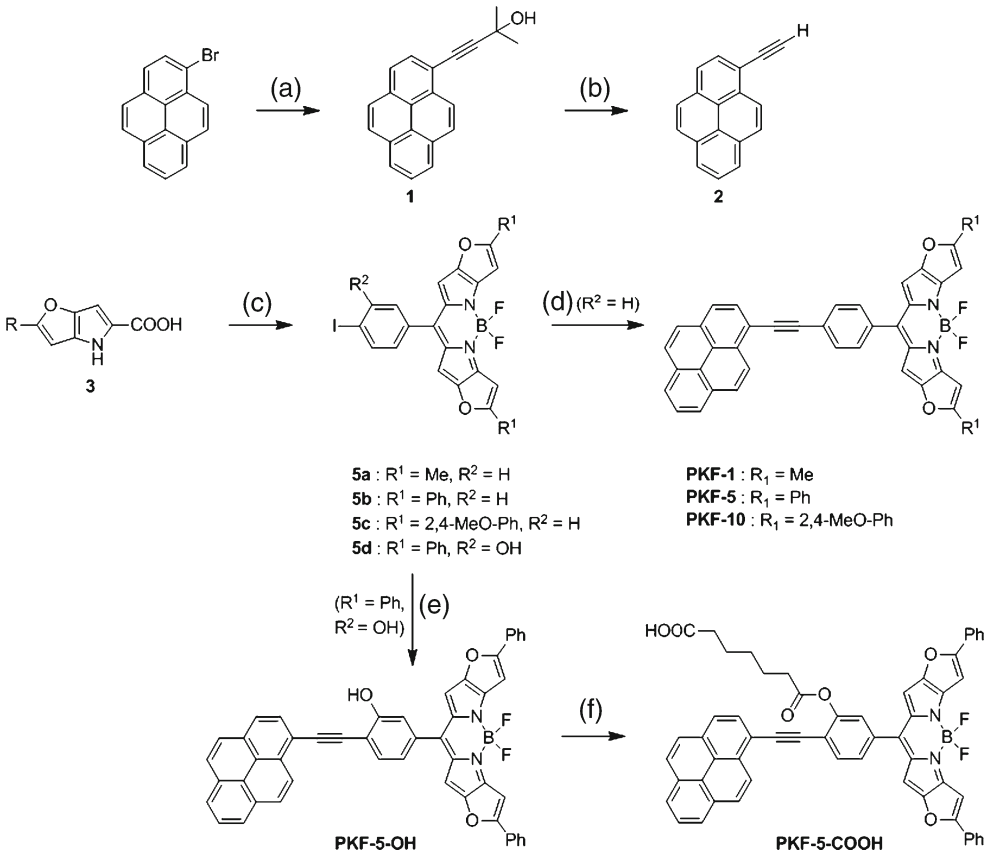

Fig. 2 Synthetic scheme for PFK series. Reagents and conditions: (a) 2-methyl-3-buten-2-ol, $PdCl_2dppf/PPh_3$, CuI, TEA, toluene; (b) KOH, toluene; (c) i) TFA, rt–50 °C; ii) 4-iodobenzaldehyde or 3-hydroxy-4-iodobenzaldehyde, TFA, $MeSO_3H$, rt, overnight, iii) *p*-chloranil, 1.5–3 h, iv) TEA or DEIA, BF_3 ether complex, CH_2Cl_2, rt, 0.5–2 h; (d) 2, $Pd(PPh_3)_4$, CuI, DIEA or TEA, DMF or 1,4-dioxane, rt, 2.5–4.5 h; (e) 2, $PdCl_2(PPh_3)_2$, CuI, TEA, THF, 45 °C, 1.5 h; (f) pimelic acid, DCC, DMAP, THF, rt, 1 h

Indeed, a similar "unexpected" fluorescence quenching was reported in some cases (e.g. fluorescein–BODIPY [18], fluorene–BODIPY dyads [29]). However, no possible mechanism of this phenomenon has been proposed yet. This implies that a complicated correlation between chemical structures of dyads and their fluorescence quantum yields would make the explanation in a simple photophysical/photochemical manner difficult, similar to our case. The moderate P_{ET} values of PKFs (PKF-5: 50 %, PKF-10: 38 %, respectively), although not quantitative unlike in the case of some pyrene–BODIPY dyads [12], result in sufficient fluorescence quantum yields of PKF-5 and -10 excited at 365 nm ($\phi_{D\text{-}A}$: 43 % and 25 %, respectively) for bioimaging applications. Furthermore, the

Table 1 Optical properties of PKFs in chloroform

	λ_{abs} [nm]	λ_{flu} [nm]	(quasi-)Stokes shift [nm]	$\Delta\lambda_{1/2}$[a] [nm]	ϕ[b] [%]	τ[c] [ns]	ε [$M^{-1}cm^{-1}$]	P_{ET}[d] [%]
PKF-1	584	599	15	22	28	1.0	141,000	
	365		234		19	1.1	41,100	68
PKF-5	656	671	15	25	86	4.0	160,000	
	371		300		43	4.0	40,000	50
PKF-10	698	719	21	32	65	3.9	159,000	
	384		335		25	4.0	40,400	38
PKF-5-COOH[e]	660	677	17	29	39	2.6	118,000	
	370		307		27	2.5	31,300	69

[a] Full width at half maximum height

[b] Fluorescence quantum yield of the acceptor unit obtained by excitation of the KFL ($\phi_{A\text{-}A}$, upper) or pyrene ($\phi_{D\text{-}A}$, lower) fragment

[c] Fluorescence lifetime

[d] Energy transfer efficiency calculated by the following equation reported in the literature: $P_{ET}=\phi_{D\text{-}A}/\phi_{A\text{-}A}$ [9]

[e] In DMSO

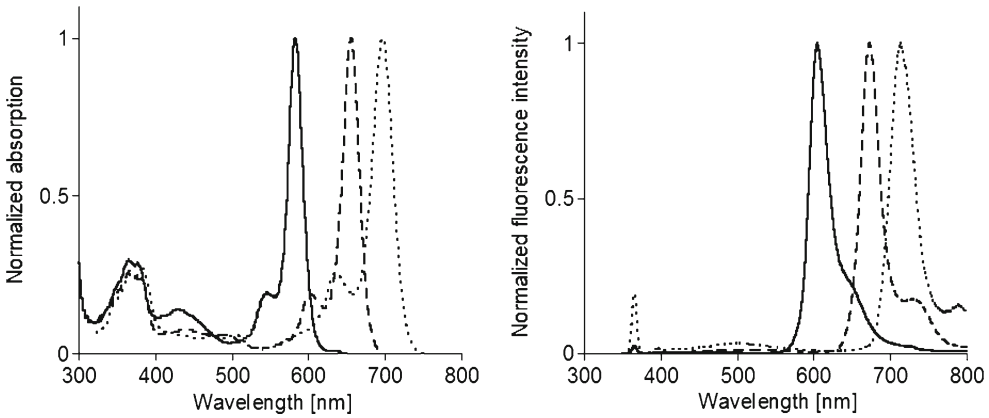

Fig. 3 Normalized absorption (*left*) and fluorescence emission (*right*) spectra of PKF-1 (*solid line*), -5 (*dashed line*), and -10 (*dotted line*) in chloroform. Excitation: 365 nm

molecular weights of the PKF dyes (<1,000 Da) are close to those of commercial fluorescent labels and probes for bioimaging such as CyDye, Atto dyes, Alexa dyes.

Synthesis and Optical Properties of PKF Labels for Bioimaging Application

On the basis of these results, focus was set on the design and synthesis of a fluorescent label having a carboxyl group that can be attached to biomolecules for practical bioimaging purposes. As the fluorescent dyad, PKF-5 was selected for this application owing to its large quasi-Stokes shift, bright emission, and compatibility with the microscopy emission filter set for Cy5. Because of the large "spectral window" of PKF-5, a variety of commercially available UV-excitable/VIS-emissive fluorescent probes and fluorescent proteins, which are widely used in bioanalytical and bioimaging studies are compatible for application in combination with PKF-5: e.g. Alexa Fluor 350 (for protein labeling), DAPI (for nuclei), Lysotracker Blue (for lysosomes), ER-tracker Blue-White (for the endoplasmic reticulum), fura-2 or indo-1 (for Ca^{2+} imaging) [30].

PKF-5-COOH shows pyrene- and KFL-derived absorption peaks (370 nm, 660 nm, respectively), as well as an emission peak corresponding to KFL (677 nm, Table 1). The fluorescence quantum yields of PKF-5-COOH excited at the pyrene ($\phi_{D\text{-}A}$) or the KFL fragment ($\phi_{A\text{-}A}$) are similar to that of other popular commercial fluorescent labels such as Cy5 (~0.2) [31]. In order to confirm the labeling applicability of PKF-5-COOH, bovine serum albumin (BSA), a widely chosen protein model, was labeled with PKF-5-COOH. The purified PKF-5-BSA conjugate exhibited intense emission (λ_{max}: 678 nm) upon excitation at 365 nm (Fig. 6), indicating the possibility of orthogonal imaging with commercially available probes.

Simultaneous Dual-Color Imaging with PKF and Fura-2 by Single-Wavelength Excitation

Finally, as proof of concept for simultaneous imaging, labeled BSA was co-imaged together with another species, such as the calcium ion (Ca^{2+}), which plays a vital role in nearly every aspect of cellular life [32]. In fact, a correlation between the behavior of serum albumin (SA) in the cell and concentration changes of species such as intracellular calcium ions ($[Ca^{2+}]_i$) has been reported in the literature [33, 34]. Hence the demonstration of simultaneous monitoring of proteins such as albumin and ions such as Ca^{2+} is considered to be a suitable fundamental model for a proof of concept. In this study, fura-2 for Ca^{2+} imaging was chosen owing to its UV-excitable property (340 or 380 nm) and visible emission peak (~510 nm), as well as its widespread

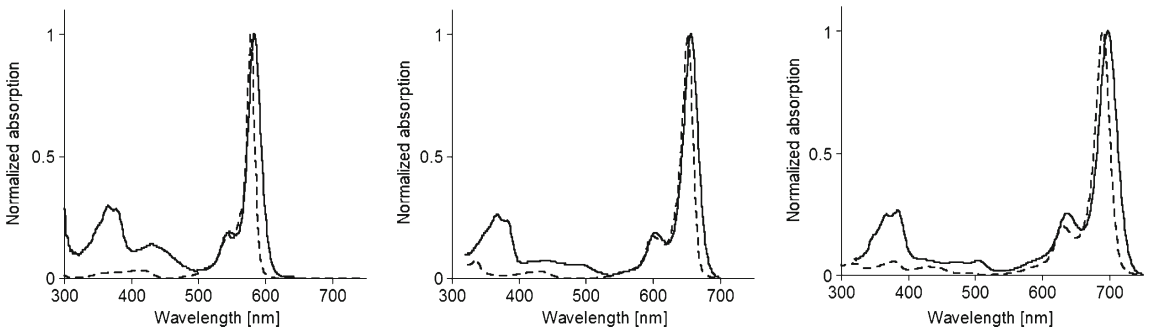

Fig. 4 Normalized absorption spectra of PKFs (*solid line*) and KFLs (*dashed line*) dyes. (*left*: PKF-1/KFL-1, *middle*: PKF-5/KFL-5, *right*: PKF-10/KFL-10)

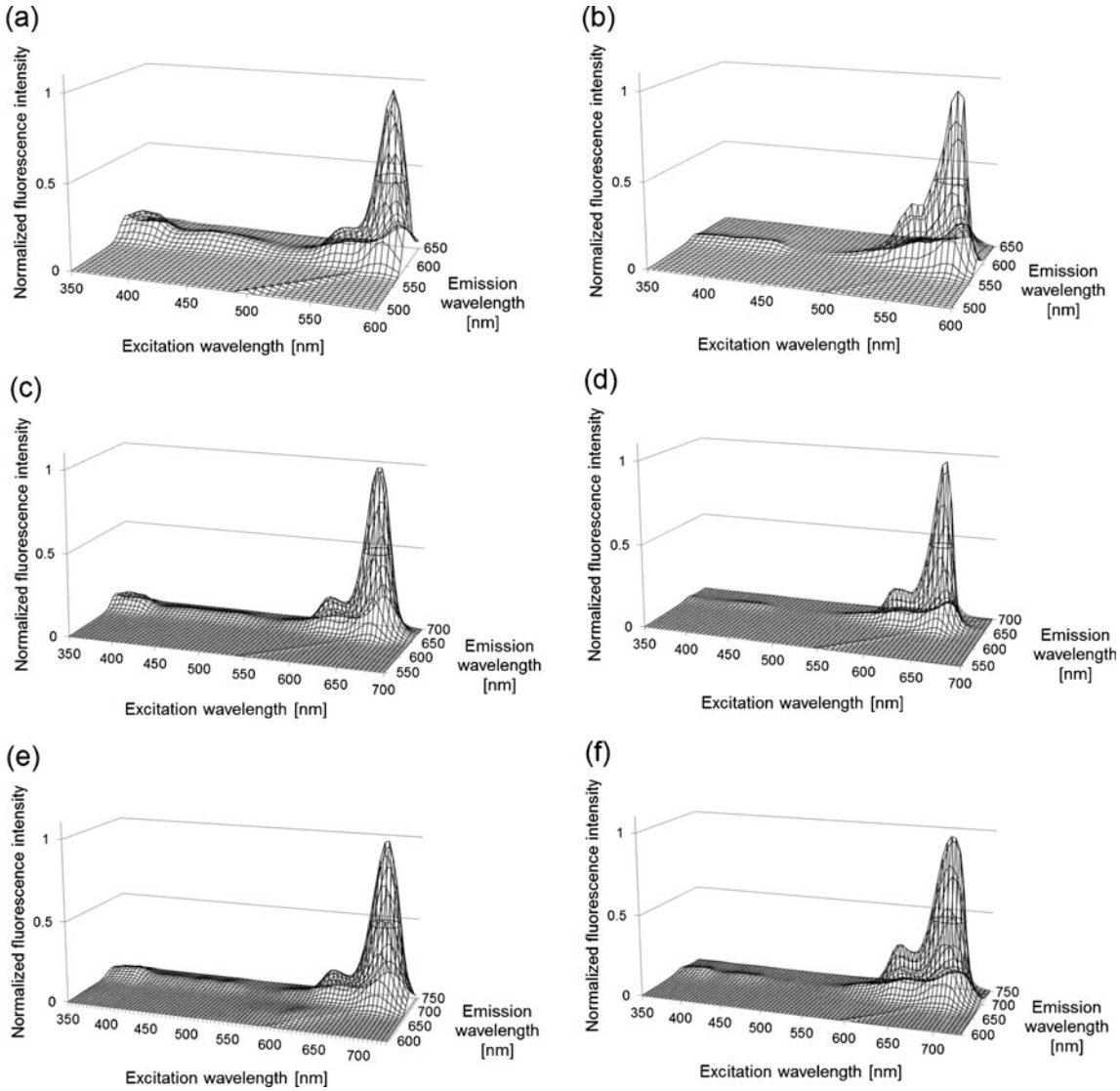

Fig. 5 Normalized 3D excitation/emission spectra of PKFs and KFLs in chloroform. **a** PKF-1, **b** KFL-1,**c** PKF-5, **d** KFL-5, **e** PKF-10, **f** KFL-10

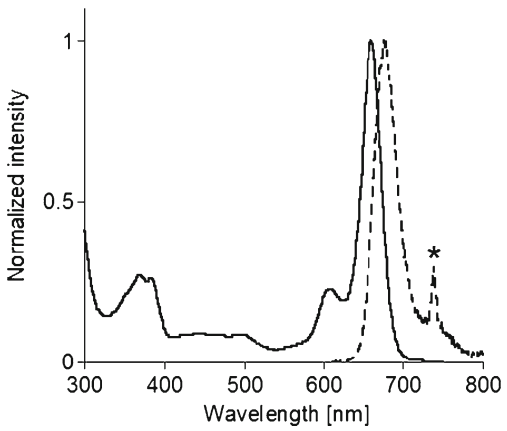

Fig. 6 Normalized absorption (*solid line*) and emission (*dashed line*) spectra of PKF-5-BSA conjugate in 0.1 M PBS buffer (pH 7.4). Excitation: 365 nm. The *spike marked with an asterisk* denotes a second-order diffraction peak of the excitation light

use for Ca^{2+} imaging [35, 36]. UV-excitable fluorescent probes such as fura-2 and Sirius [1] (blue fluorescent protein) are nowadays recognized as useful tools and widely applied for multicolor intracellular imaging, despite of some potential phototoxicity issues caused by UV light. In analogy, the useful optical properties of the PKF probes are believed to be sufficiently advantageous to compensate the potential disadvantages of UV-excitation. The excitation efficiency of fura-2 at 380 nm decreases with increasing Ca^{2+} concentration, resulting in a decreasing fluorescence emission intensity at 510 nm [35]. Therefore, the excitation wavelength was set at 380 nm, and the following emission filters were used: 535 nm/55 nm band-pass filter for fura-2, and 600 nm long-pass filter for PKF.

After incubation of HUVEC cells (a well-known type of endothelial cells) in the presence of PKF-5-BSA conjugate

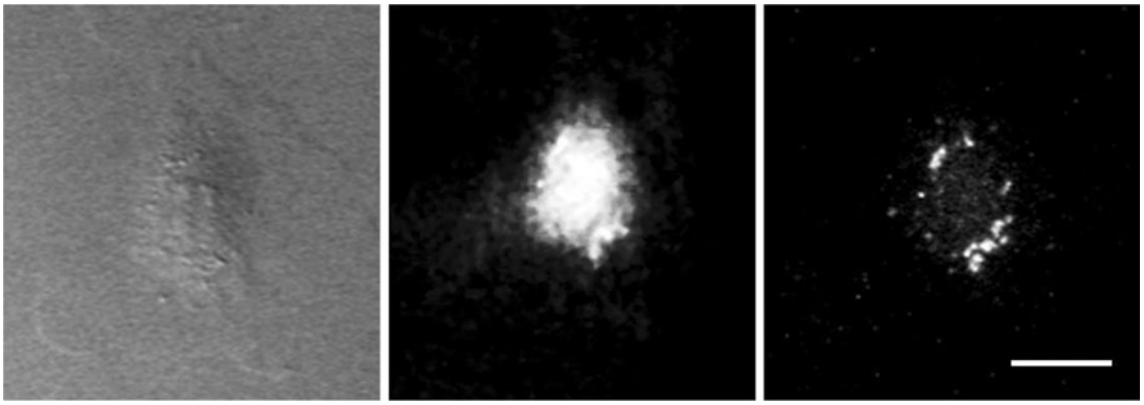

Fig. 7 Bright field image (*left*) and fluorescence images (*middle* and *right*) of HUVEC cells loaded with both PKF-5-BSA conjugate (*middle*) and fura-2 (*right*). Excitation: 380 nm. Scale bar: 20 μm

and fura-2 acetoxymethyl (AM) ester in culture buffer, both of label and probe were successfully taken up into the HUVEC cells as shown in Fig. 7. In this experiment, PKF was used as a marker (not as an indicator) for visualizing and trafficking a protein of interest incorporated in cells, while fura-2 was used as a Ca^{2+} indicator of Ca^{2+} in cytoplasm. Therefore the two compounds (PKF and fura-2) are expected to behave independently of each other inside cells, resulting in simultaneous imaging of protein trafficking (by PKF) and change of Ca^{2+} concentration (by fura-2). The fluorescence emission captured through the filter for fura-2 (Fig. 7, middle) or for PKF-5 (Fig. 7, right) showed that both signals could be simultaneously and independently observed in each channel with good signal separation by single irradiation of 380 nm excitation light (PKF: dot-like signal, fura-2: distributed signal). This result is fully consistent with the above-mentioned expectations. Although autofluorescence of intracellular species (e.g. NADH) by UV excitation potentially increases the level of background fluorescence, no emission signal assigned to background was observed during our experiments due to the strong emission intensity of fura-2.

As a further application demonstration, simultaneous real-time imaging of BSA and Ca^{2+} was undertaken. After ATP stimulation of the cells causing an increase of $[Ca^{2+}]_i$ [28], the fluorescence emission signal of fura-2 (510 nm) decreased, whereas that of PKF did not fluctuate (Fig. 8). Although this is just a preliminary demonstration model, the results indeed reveal the possibility of real-time simultaneous dual-color imaging of two intracellular species with single wavelength excitation.

Conclusions

The newly designed and synthesized fluorescent PFK dyads enabled simultaneous dual-color imaging of two different species in cells by single-wavelength excitation. These results from fundamental design to practical application not only prove the applicability of the novel fluorescent cassettes for bioimaging, but also suggest ideas for further applications. For instance, the flexible molecular design and the modification possibilities of organic compounds, which are among the biggest advantages compared to using protein-based FRET sensors, will help to develop functional fluorescent molecular dyads, such as fluoroionophores [30], and site-specific labels (SNAP/CLIP-tag [37, 38], HaloTag [39], oligo-Asp-tag [40]) among others.

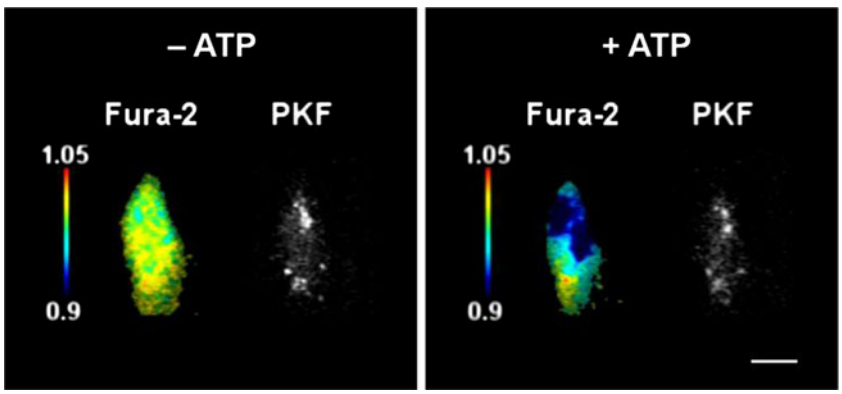

Fig. 8 Real-time fluorescence images of HUVEC cells co-loaded with Fura-2 (for Ca^{2+} sensing) and PKF (for tracing albumin) before (*left*) and after (*right*) ATP stimulation. Excitation: 380 nm. Dichroic mirror: 590 nm. Filter for emission signal: 535/55 band pass filter (for Fura-2), 600 nm long pass filter (for PKF). Scale bar: 20 μm

Acknowledgement We acknowledge T. Shichi (Nissan Arc. Ltd.) for his help with ESI-MS data acquisition, and Y. Urano (The University of Tokyo) for his support for fluorescence lifetime measurements. This work was supported by a JSPS stipend to K.U. and a Grant-in-Aid for Scientific Research (A) from the Ministry of Education, Culture, Sports, Science and Technology, Japan (No. 20245019).

References

1. Tomosugi W, Matsuda T, Tani T, Nemoto T, Kotera I, Saito K, Horikawa K, Nagai T (2009) An ultramarine fluorescent protein with increased photostability and pH insensitivity. Nat Methods 6(5):351–353
2. Niino Y, Hotta K, Oka K (2009) Simultaneous live cell imaging using dual FRET sensors with a single excitation light. PLoS One 4(6):e6036
3. Weissleder R (2001) A clearer vision for in vivo imaging. Nat Biotechnol 19(4):316–317
4. Zhao Q, Huang C, Li F (2011) Phosphorescent heavy-metal complexes for bioimaging. Chem Soc Rev 40(5):2508–2524
5. Ziessel R, Harriman A (2011) Artificial light-harvesting antennae: electronic energy transfer by way of molecular funnels. Chem Commun 47(2):611–631
6. Harriman A, Izzet G, Ziessel R (2006) Rapid energy transfer in cascade-type bodipy dyes. J Am Chem Soc 128(33):10868–10875
7. Ulrich G, Ziessel R, Harriman A (2008) The chemistry of fluorescent bodipy dyes: versatility unsurpassed. Angew Chem Int Ed 47(7):1184–1201
8. Ulrich G, Goze C, Guardigli M, Roda A, Ziessel R (2005) Pyrromethene dialkynyl borane complexes for cascatelle energy transfer and protein labeling. Angew Chem Int Ed 44(24):3694–3698
9. Goze C, Ulrich G, Ziessel R (2007) Tetrahedral boron chemistry for the preparation of highly efficient "Cascatelle" devices. J Org Chem 72(2):313–322
10. Goeb S, Ziessel R (2007) Convenient synthesis of green diisoindolodithienylpyrromethene-dialkynyl borane dyes. Org Lett 9(5):737–740
11. Harriman A, Mallon LJ, Goeb S, Ulrich G, Ziessel R (2009) Electronic energy transfer to the S_2 level of the acceptor in functionalised boron dipyrromethene dyes. Chem Eur J 15(18):4553–4564
12. Ulrich G, Goeb S, De Nicola A, Retailleau P, Ziessel R (2011) Chemistry at boron: synthesis and properties of red to near-IR fluorescent dyes based on boron-substituted diisoindolomethene frameworks. J Org Chem 76(11):4489–4505
13. Coskun A, Akkaya EU (2006) Signal ratio amplification via modulation of resonance energy transfer: proof of principle in an emission ratiometric Hg(II) sensor. J Am Chem Soc 128(45):14474–14475
14. Wu L, Loudet A, Barhoumi R, Burghardt RC, Burgess K (2009) Fluorescent cassettes for monitoring three-component interactions in vitro and in living cells. J Am Chem Soc 131(26):9156–9157
15. Lin W, Yuan L, Cao Z, Feng Y, Song J (2010) Through-bond energy transfer cassettes with minimal spectral overlap between the donor emission and acceptor absorption: Coumarin–rhodamine dyads with large pseudo-Stokes shifts and emission shifts. Angew Chem Int Ed 49(2):375–379
16. Jiao GS, Thoresen LH, Burgess K (2003) Fluorescent, through-bond energy transfer cassettes for labeling multiple biological molecules in one experiment. J Am Chem Soc 125(48):14668–14669
17. Bandichhor R, Petrescu AD, Vespa A, Kier AB, Schroeder F, Burgess K (2006) Water-soluble through-bond energy transfer cassettes for intracellular imaging. J Am Chem Soc 128(33):10688–10689
18. Thivierge C, Han J, Jenkins RM, Burgess K (2011) Fluorescent proton sensors based on energy transfer. J Org Chem 76(13):5219–5228
19. Loudet A, Bandichhor R, Wu LX, Burgess K (2008) Functionalized BF_2 chelated azadipyrromethene dyes. Tetrahedron 64(17):3642–3654
20. Jose J, Ueno Y, Castro JC, Li L, Burgess K (2009) Energy transfer dyads based on Nile Red. Tetrahedron Lett 50(47):6442–6445
21. Ueno Y, Jose J, Loudet A, Pérez-Bolívar CS, Anzenbacher P, Burgess K (2010) Encapsulated energy-transfer cassettes with extremely well resolved fluorescent outputs. J Am Chem Soc 133(1):51–55
22. Loudet A, Ueno Y, Wu L, Jose J, Barhoumi R, Burghardt R, Burgess K (2011) Organelle-selective energy transfer: a fluorescent indicator of intracellular environment. Bioorg Med Chem Lett 21(6):1849–1851
23. Umezawa K, Matsui A, Nakamura Y, Citterio D, Suzuki K (2009) Bright, color-tunable fluorescent dyes in the vis/NIR Region: establishment of new "tailor-made" multicolor fluorophores based on borondipyrromethene. Chem Eur J 15(5):1096–1106
24. Eaton DF (1988) Reference materials for fluorescence measurement. Pure Appl Chem 60(7):1107–1114
25. Magde D, Brannon JH, Cremers TL, Olmsted J (1979) Absolute luminescence yield of cresyl violet. A standard for the red. J Phys Chem 83(6):696–699
26. Dempster DN, Morro T, Rankin R, Thompson GF (1972) Photochemical characteristics of cyanine dyes. 1. 3,3′-Diethyloxadicarbocyanine iodide and 3,3′-diethylthiadicarbocyanine iodide. J Chem Soc, Faraday Trans 2 68(9):1479–1496
27. Umezawa K, Nakamura Y, Makino H, Citterio D, Suzuki K (2008) Bright, color-tunable fluorescent dyes in the visible-near-infrared region. J Am Chem Soc 130(5):1550–1551
28. Matsui A, Umezawa K, Shindo Y, Fujii T, Citterio D, Oka K, Suzuki K (2011) A near-infrared fluorescent calcium probe: a new tool for intracellular multicolour Ca^{2+} imaging. Chem Commun 47(37):10407–10409
29. Thivierge C, Loudet A, Burgess K (2011) Brilliant BODIPY −fluorene copolymers with dispersed absorption and emission maxima. Macromolecules 44(10):4012–4015
30. Haugland RP (2005) The Handbook: a guide to fluorescent probes and labeling technologies. Invitrogen Corp, Eugene
31. GE Healthcare Bioscience catalogue (2006) GE Healthcare UK Ltd., Amersham
32. Clapham DE (2007) Calcium signaling. Cell 131(6):1047–1058
33. Carter DC, Ho JX (1994) Structure of serum albumin. Adv Protein Chem 45:153–203
34. Fuentes E, Nadal A, Jacob R, McNaughton P (1997) Actions of serum and plasma albumin on intracellular Ca^{2+} in human endothelial cells. J Physiol 504(Pt 2):315–326
35. Grynkiewicz G, Poenie M, Tsien RY (1985) A new generation of Ca^{2+} indicators with greatly improved fluorescence properties. J Biol Chem 260(6):3440–3450
36. Carlson HJ, Campbell RE (2009) Genetically encoded FRET-based biosensors for multiparameter fluorescence imaging. Curr Opin Biotechnol 20(1):19–27
37. Keppler A, Gendreizig S, Gronemeyer T, Pick H, Vogel H, Johnsson K (2003) A general method for the covalent labeling of fusion proteins with small molecules in vivo. Nat Biotechnol 21(1):86–89

38. Gautier A, Juillerat A, Heinis C, Correa IR, Kindermann M, Beaufils F, Johnsson K (2008) An engineered protein tag for multiprotein labeling in living cells. Chem Biol 15(2):128–136
39. Los GV, Encell LP, McDougall MG, Hartzell DD, Karassina N, Zimprich C, Wood MG, Learish R, Ohana RF, Urh M, Simpson D, Mendez J, Zimmerman K, Otto P, Vidugiris G, Zhu J, Darzins A, Klaubert DH, Bulleit RF, Wood KV (2008) HaloTag: a novel protein labeling technology for cell imaging and protein analysis. ACS Chem Biol 3(6):373–382
40. Ojida A, Honda K, Shinmi D, Kiyonaka S, Mori Y, Hamachi I (2006) Oligo-Asp Tag/Zn(II) complex probe as a new pair for labeling and fluorescence imaging of proteins. J Am Chem Soc 128(32):10452–10459